Polymer Degradation and Stability 94 (2009) 651–658

Contents lists available at ScienceDirect

Polymer Degradation and Stability

journal homepage: www.elsevier.com/locate/polydegstab

Surface molecular characterisation of different epoxy resin composites subjected to UV accelerated degradation using XPS and ToF-SIMS

Firas Awaja [a,*], Paul J. Pigram [b,c]

[a] Centre for Material and Fibre Innovation, Geelong Technology Precinct, Deakin University, Geelong, Victoria 3217, Australia
[b] Centre for Materials and Surface Science, La Trobe University, Victoria 3086, Australia
[c] Department of Physics, La Trobe University, Victoria 3086, Australia

ARTICLE INFO

Article history:
Received 10 November 2008
Accepted 2 January 2009
Available online 14 January 2009

Keywords:
ToF-SIMS
XPS
Accelerated degradation
Epoxy resin
UV

ABSTRACT

Epoxy resin composites reinforced with E-glass (E), 3D glass (3D) and carbon fibre (CF) were subjected to an intense UV and high temperature accelerated degradation environment. X-ray photoelectron spectroscopy (XPS) and time-of-flight secondary ion mass spectrometry (ToF-SIMS) were used to provide a molecular characterisation of the surface of the degraded composites. The response at the surface of the epoxy resin composites to oxidative degradation is influenced by the composite reinforcement type and characteristics. XPS results indicate that 3D resin composites exhibit more surface oxidation as a result of the accelerated degradation in comparison with E and CF composites. Principal components analysis (PCA) of the ToF-SIMS positive ion spectra showed that E and 3D resin composites suffered chain scission while CF composites suffered chain scission and cross-linking reactions as a result of the intense UV exposure. The extent of the surface oxidation, cross-linking/condensation reaction and loss of low molecular weight (lower than C_4H_x) aliphatic hydrocarbons may be indicated using PCA of both the ToF-SIMS positive and negative ion spectra. PCA also provides insight for proposing epoxy resin chain scission and oxidation reaction mechanisms.

1. Introduction

Glass and carbon fibre reinforced epoxy resin composites are used in many applications due to their favourable mechanical properties and performance under harsh environmental conditions [1–3]. The surfaces of epoxy resin composites often degrade under conditions that induce chemical and physical changes such as sunlight, oxidation and other external agents [4,5]. Understanding the chemical and physical changes of the degraded surfaces will allow tailoring of these materials for better performance under severe ultraviolet (UV) and temperature conditions.

Solar UV radiation in the presence of oxygen generates a strong thermal and oxidative degradation force for polymer composites [4,5]. Oxidative thermal degradation at the surface of epoxy resin composites leads to structural damage as a result of thermal-mechanical stress and oxidation effects [5–7]. Thermal stress generates mechanical pressure at the surface and in the bulk resulting in crack initiation and propagation. Surface oxidation at elevated temperatures results in an increase in surface density due to outgassing of volatiles and shrinkage. The latter also leads to the generation of cracks [6,8,9]. Cracking is the major cause of polymer composite failure. It is frequently difficult to detect and the associated structural fragmentation leads to reductions in strength, stiffness and dimensional stability [10–15]. Further, cracks, structural defects and delamination that form deep within the structure of syntactic foam are extremely difficult to detect and repair [11]. These internal defects not only decrease the polymer composite performance but also serve as catalysts for further damage including macrocracks [10], moisture swelling and debonding [11]. It has been reported that the epoxy resin composite failure commonly occurs as a single layer breakdown, for example, cracking of the embedded fibres or the epoxy resin. Fibre elastic buckling and separation from the resin matrix have also been reported as typical composite failure modes [12,13].

The surface properties of epoxy resin composites have been linked previously to the nature of the reinforcement fibre [16,17]. Bénard et al. [16] reported that surface chemical composition, roughness and adhesion strength of epoxy resin composites depend on the fibre characteristics. The reduction in polymer composite mechanical properties as a result of thermal aging is reported to be

* Corresponding author. Present address: School of Physics, University of Sydney, Sydney, NSW 2006, Australia. Fax: +613 9479 1552.
E-mail address: firas@physics.usyd.edu.au (F. Awaja).

0141-3910/$ – see front matter © 2009 Elsevier Ltd. All rights reserved.
doi:10.1016/j.polymdegradstab.2009.01.001

dependent on the interface between the re-enforcement filler and the resin matrix [17]. Ray [17] also reported that weight loss in a glass and carbon fibre epoxy composite which had undergone thermal aging in humid conditions was dependent on the interface state of the composite. Other researchers reported that the geometry of the polymer composite fillers has a significant effect on the ability of the composite to sustain impact without significant damage [18]. Local thermal stresses are generated due to different thermal expansion behaviour between the filler and the resin matrix [19].

Time-of-flight secondary ion mass spectrometry (ToF-SIMS) is a surface sensitive technique with the ability to provide in-depth information about the surface composition, molecular structure and chemical bonding of materials [20–24]. However, the ionisation processes occurring in ToF-SIMS are complex and hence direct quantification is difficult. Multivariate calibration methods such as principal components analysis (PCA) are commonly used to assist with data interpretation. X-ray photoelectron spectroscopy (XPS), in comparison, provides quantitative relative surface composition information through the use of photoelectron peak intensities and corresponding empirical relative sensitivity factors. XPS and ToF-SIMS are well suited for use in combination to characterise surface chemistry at the molecular level [22,24–27].

This study examines surface molecular changes of epoxy composites, with different reinforcements, in response to intense ultraviolet irradiation and high temperature. The surface degradation behaviour is explored using XPS and ToF-SIMS techniques.

2. Experimental

2.1. Materials

KINETIX R246TX epoxy resin (ATL Composites, Australia) was used in this study, consisting of a diglycidyl ether of bisphenol A (DGEBA)/diglycidyl ether of bisphenol F (DGEBF) resin blend with an aliphatic glycidyl ether functional diluent. Super fast hardener, KINETIX H126 (ATL Composites, Australia), manufactured to cure at room temperature is an aliphatic/cycloaliphatic amine, with isophorone diamine (IPD) being the main ingredient. Three types of reinforcement were selected for testing. These included a stitched non-crimp double bias E-glass (ATL Composites, Australia) (E composite), a stitched non-crimp carbon fibre (formax FCIM136, 12k 451GSM −45/+45) (CF composite) and a 3D woven glass known as Parabeam™ Para 12 mm (ATL Composites, Australia) (3D composite).

The Kinetix epoxy resin system was mixed at a ratio of 4 parts resin to 1 part hardener based on the manufacturer's recommendations. The resin was then degassed at full vacuum for 15 min prior to infusion. The infusion took place at room temperature and was allowed to cure overnight before being debagged and trimmed. The cured panels were then placed in an oven and post-cured for 4 h at 100 °C. Each of the reinforcements was cut and assembled in as close to a quasi-isotropic lay-up as possible, depending on the number of layers used in each laminate, to maintain a similar cured composite thickness for each. The stacking sequence for the E-glass composites was 8 layers at total thickness of 2.97 mm, 8 layers with total thickness of 3.77 mm for the carbon fibre composite and 2 layers with total thickness of 2.98 mm for the Parabeam 3D glass composite.

2.2. UV degradation chamber

The accelerated degradation chamber has an UV source and a heated sample tray. The sample tray has an area of 500 × 250 mm. UV illumination is provided via two OSRAM Ultravitalux 300 W sun lamps, containing a quartz discharge tube and tungsten filament in a high pressure bulb. The bulb contains a reflector and the glass is doped to ensure that the lamp emits only the UVA and UVB radiation contained in sunlight. The area of the sample tray is illuminated by two of these bulbs at a distance of 500 mm from the tray, the irradiation level is 1 kW m^{-2}. The surface temperature of the sample tray is 95 °C, controlled with a temperature controller, cooling fan at the roof of the chamber, and a thermocouple on the sample tray for temperature feedback.

2.3. XPS

XPS measurements were performed using an Axis Ultra DLD spectrometer (Kratos Analytical, UK), equipped with a monochromatic X-ray source (Al Kα, $h\nu = 1486.6$ eV) operating at 150 W. Three replicate tests were used for each sample. The spectrometer energy scale was calibrated using the Au $4f_{7/2}$ photoelectron peak at binding energy $E_B = 83.98$ eV. Survey spectra were acquired for binding energies in the range 0–1400 eV, using a pass energy of 160 eV. C 1s, O 1s and N 1s region spectra were acquired at a pass energy of 20 eV to obtain higher spectral resolution. Peaks were fitted with synthetic Gaussian (70%)–Lorentzian (30%) components using the Marquardt–Levenberg fitting procedure of CasaXPS and were quantified using relative sensitivity factors supplied by the spectrometer manufacturer. Linear background subtraction was used and the spectra were charge corrected by setting the C 1s C–C/H component to 285.0 eV [28]. The analysis area was approximately 700 μm × 300 μm.

2.4. ToF-SIMS

ToF-SIMS analyses were performed using a ToF-SIMS IV instrument (Ion-TOF GmbH, Germany) equipped with a reflectron time-of-flight mass analyzer, a Bi_3^+ cluster ion source (25 keV) and a pulsed electron flood source for charge compensation. The primary pulsed ion beam current was 1.1 pA and the primary ion dose density was below the static SIMS limit of 10^{13} ions cm^{-2}. Positive ion mass spectra were acquired from a minimum of five 100 μm × 100 μm areas from each sample using a cycle time of 100 μs. Mass resolution was greater than 7500 at $m/z = 29$.

2.5. Data analysis

The peaks for data analysis were selected initially based on reference libraries and previous assignments in the literature for DGEBA, DGEBF and IPD molecules [29–32]. Further peaks were assigned using the library and the exact mass calculator tool incorporated in the Ionspec software package (Ion-TOF GmbH, Germany) to identify contaminant peaks, including hydrocarbon peaks, and peaks that were likely to correspond to fragments of the resin/hardener not listed in the literature. All the significant peaks above baseline in the m/z range from 0 to 350 were selected. There was no significant peaks were observed above 350 m/z other than common contamination peaks in the range of 350–600 m/z. The mass spectra were calibrated using a series of hydrocarbon (C_xH_y) peaks up to $m/z = 105$.

The data were grouped in a matrix and mean-centred. The columns in the matrix were normalised to the total intensity before mean centring. The mean-centred matrix was used for PCA. PCA is a multivariate technique used to assist the interpretation of large datasets such as those generated by ToF-SIMS, in particular, identifying meaningful variables describing the major physical phenomena in the system. PCA was performed using code developed in-house based on the covariance method algorithm described in detail by Martens and Naes [33].

3. Results and discussion

XPS was used to survey the distribution of species at the surface of all composite samples (Table 1), giving an indication of the extent of surface oxidation. The 3D glass sample surface oxygen content was significantly increased (~50%) due to the accelerated degradation conditions. The E-glass and CF composite oxygen content also increased but by a lesser amount (by about 30%) as a result of the treatment. All samples showed a significant increase in nitrogen concentration at the surface. The 3D glass composite showed the greatest increase in N and the greatest decrease in C at the surface as a result of the treatment. The O/C ratio for all composites increased significantly (Table 1), indicating that surface oxidation is the dominant process resulting from UV treatment.

Table 2 shows the assignment of component peaks corresponding to surface functional groups for the XPS region scans. For the C 1s region scans, all samples exhibited a significant reduction in the C–C/C–H component, consistent with chain scission. The 3D glass composite showed the highest level of chain scission (30%) followed by the CF composite (19.4%) and the E-glass composite (16%). Table 2 also shows a significant increase in the C–O/C–N functional group as a result of the treatment. The 3D glass sample showed the most significant increase (~100%) followed by the CF composite (60%) and the E-glass composite (14%). These increases in C–O concentration are attributed to surface oxidation. The component peak corresponding to carbonyl (C═O) species increased by 108% for the CF composite sample; but was unchanged for the other composites. Previous oxygen [34] and argon [35] plasma treatment studies of CF composites have reported similar surface chemical changes. Changes in the O–C═O/N–C═O molecular species did not show a clear trend among the samples. Curve fitting for the O1s region scans showed that C═O molecular species increased in relative concentration as a result of thermal treatment for all composites. The relative concentration of the C–O molecular group also increased in all samples with the 3D glass composite showing the strongest change. As expected, changes in the O–C═O functional group did not show a clear trend among the samples. Curve fitting for the N 1s region scans showed a significant increase in the N–C concentration with treatment.

ToF-SIMS positive and negative ion mass spectra were collected and pre-processed for all composite samples, before and after UV accelerated degradation treatment. PCA was used to analyse the ToF-SIMS positive ion mass spectral data of all the investigated samples. The first principal component (PC1) accounted for 81.4% of the total variance in the data. The second (PC2), third (PC3) and fourth (PC4) principal components accounted for 12.9%, 3.2%, and 1.1% variance in the data, respectively. The remaining principal components collected less than 1.4% of the total variance and were deemed insignificant. The PCA scores and loadings plots are shown in Figs. 1 and 2 respectively. Fig. 3 shows the normalised relative intensity of selected ions that showed significant variance by PCA.

Fig. 1 shows the scores plots for PC1 vs PC2. Information collected by PC1 classified the samples into three distinct groups according to their scores value. The first group contained the untreated E-glass and 3D glass samples (E-UN and 3D-UN). The second group contained the treated and the untreated carbon fibre composite samples (CF-T and CF-UN). The last group contained the treated samples of the E-glass and 3D glass samples (3D-T1,2,3 and E-T). Information collected by PC1 highlighted the significant differences between the treated and the untreated glass composite samples for both types of glass enforcements. However, there was no significant difference between the treated and the untreated CF composite samples in PC1. PC1 also showed that the CF samples are significantly different to the untreated glass composite samples but featured in close proximity with the treated glass composite samples.

Fig. 2a shows that two groups of ions appearing on opposite sides of the loadings plots play the central role in distinguishing sample types in PC1. The first and most significant group contains

Table 1
Relative atomic concentrations of elements present in the surface of epoxy resin composites after and before accelerated degradation by XPS.

Sample	C	O	N	Na	S	Si	Cl	Ca	O/C
E-untreated	79.0	15.7	1.3	3.5	0.1	0.2	0.2	0.0	0.19
E-glass treated	75.2	20.5	2.4	0.5	0.1	0.9	0.4	0.0	0.28
3D untreated	83.7	14.2	0.9	0.5	0.1	0.4	0.2	0.0	0.17
3D glass 1	73.0	21.4	3.3	1.5	0.1	0.4	0.3	0.0	0.29
3D glass 2	70.1	22.2	2.6	1.2	0.2	3.0	0.5	0.3	0.31
3D glass 3	74.0	21.0	3.2	0.8	0.1	0.5	0.3	0.0	0.28
Carbon fibre untreated	86.1	10.6	1.1	1.5	0.0	0.6	0.0	0.3	0.12
Carbon fibre treated	82.6	13.5	1.7	1.2	0.0	0.7	0.1	0.2	0.16

Table 2
Relative atomic concentrations of carbon, oxygen and nitrogen species determined from curve fitting of high resolution C 1s, O 1s and N1s XPS spectra obtained from epoxy resin composites after and before accelerated degradation.

Sample	C 1s				O 1s			N 1s
	C–C/H	C–O/C–N	C═O	O–C═O/N–C═O	C═O	C–O	O–C═O	C–N
E-untreated	57.0	18.3	4.6	3.7	4.4	7.6	2.8	1.6
E-glass treated	47.9	20.9	4.8	2.9	6.6	8.8	4.6	3.4
3D untreated	63.8	11.6	4.9	4.0	4.2	6.9	3.2	1.4
3D glass 1	40.6	26.3	4.4	3.0	6.6	12.6	2.8	3.7
3D glass 2	48.4	19.2	4.7	2.9	8.1	11.2	2.9	2.6
3D glass 3	44.2	23.6	4.4	4.0	7.2	8.8	4.4	3.6
Carbon fibre untreated	72.0	10.8	3.4	1.8	2.5	6.5	1.8	1.3
Carbon fibre treated	58.0	17.6	7.1	2.6	3.0	8.2	1.7	1.8

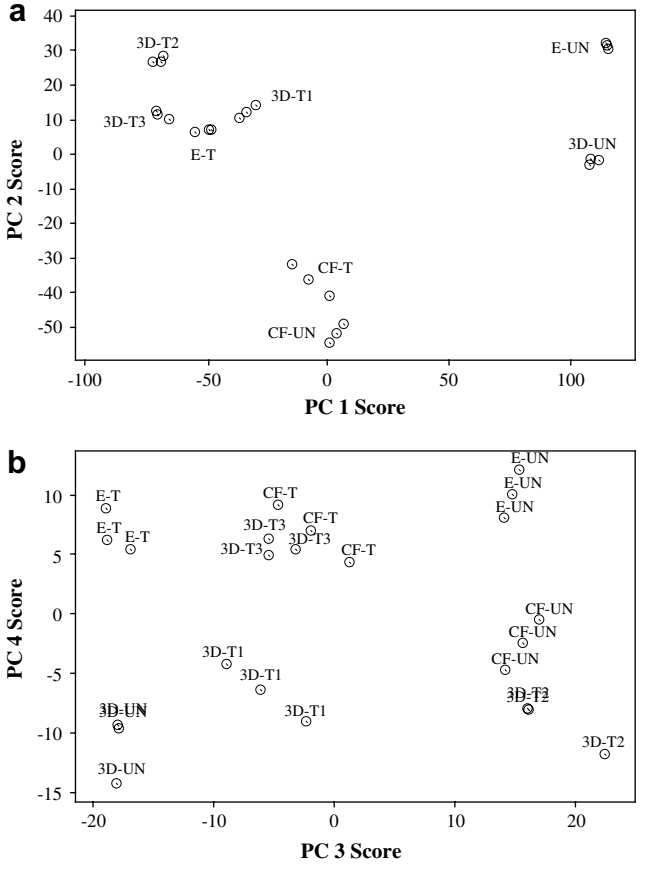

Fig. 1. Principal components analysis scores plots of the positive ToF-SIMS spectra for (a) PC1 vs PC2 score and (b) PC3 vs PC4 score.

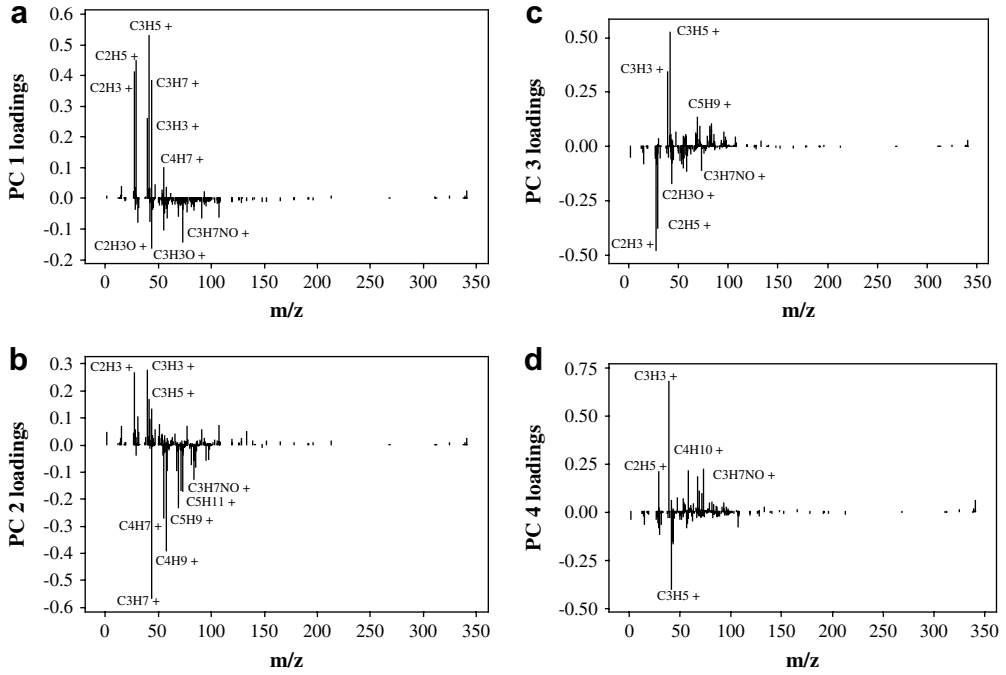

Fig. 2. Principal components analysis loadings plots for the ToF-SIMS positive spectra of (a) PC1, (b) PC2, (c) PC3 and (d) PC4.

the aliphatic hydrocarbon ions $C_3H_5^+$, $C_2H_5^+$, $C_2H_3^+$, $C_3H_7^+$, $C_3H_3^+$ and $C_4H_7^+$. Comparison between Figs. 1a and 2a indicates that the aliphatic hydrocarbon relative ion intensity is the decisive factor that distinguishes between the treated and untreated samples. These ions arise from resin chain scission resulting from the intense UV irradiation and are consistent with the earlier XPS results showing the reduction in C–C/C–H molecular groups. This is the most significant event occurring during UV degradation of the resin composites that is captured by PC1. Further, for cured epoxy resin (DEGBA/IPD), the aliphatic hydrocarbon relative ion intensity has been shown to be proportional to cross-linking density [36]. A reduction in the intensity of these ions indicates a network rupture and reduction in network density. These ions are the products of the main epoxy chain scission reactions and are mostly released as volatiles during and after the UV treatment. Fig. 4 shows a proposed DEGBA/IPD chain scission reaction mechanism based on the information provided by PC1. Initial chain breakage occurs in multiple locations generating unstable structural fragments. Further chain scission fragmentation of these structures results in low molecular weight aliphatic hydrocarbon and oxygen-containing species that may be released from the surface during the ToF-SIMS experiment. This is evident through the reduction of the

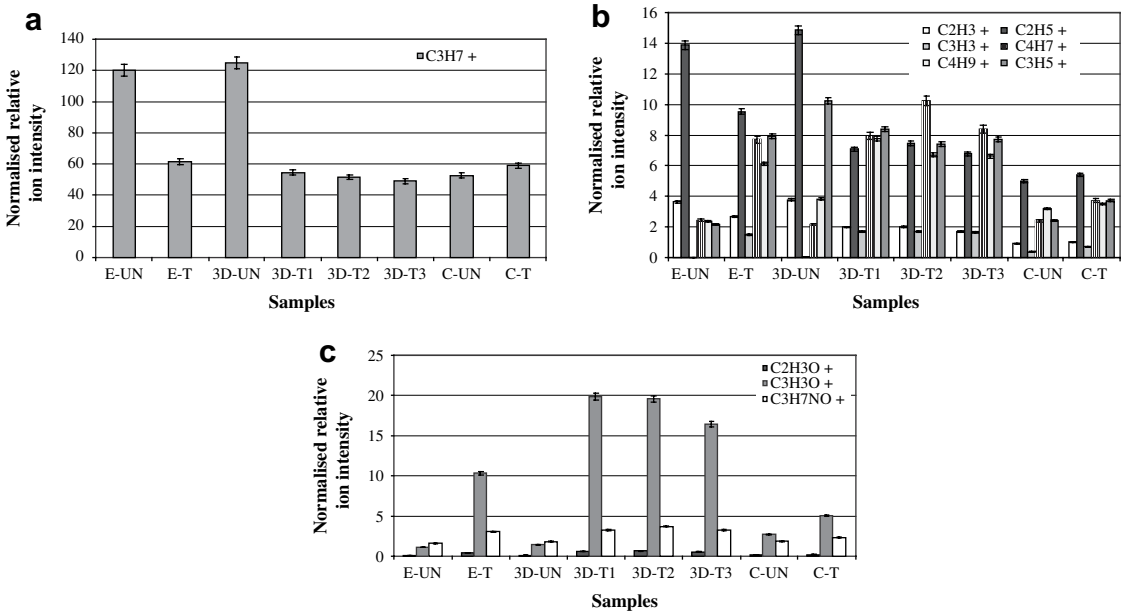

Fig. 3. Variation in the intensity of secondary ion peaks of the positive ToF-SIMS spectra that showed significant variance by PCA. Each bar represents the average of three readings of ion intensities with standard deviation.

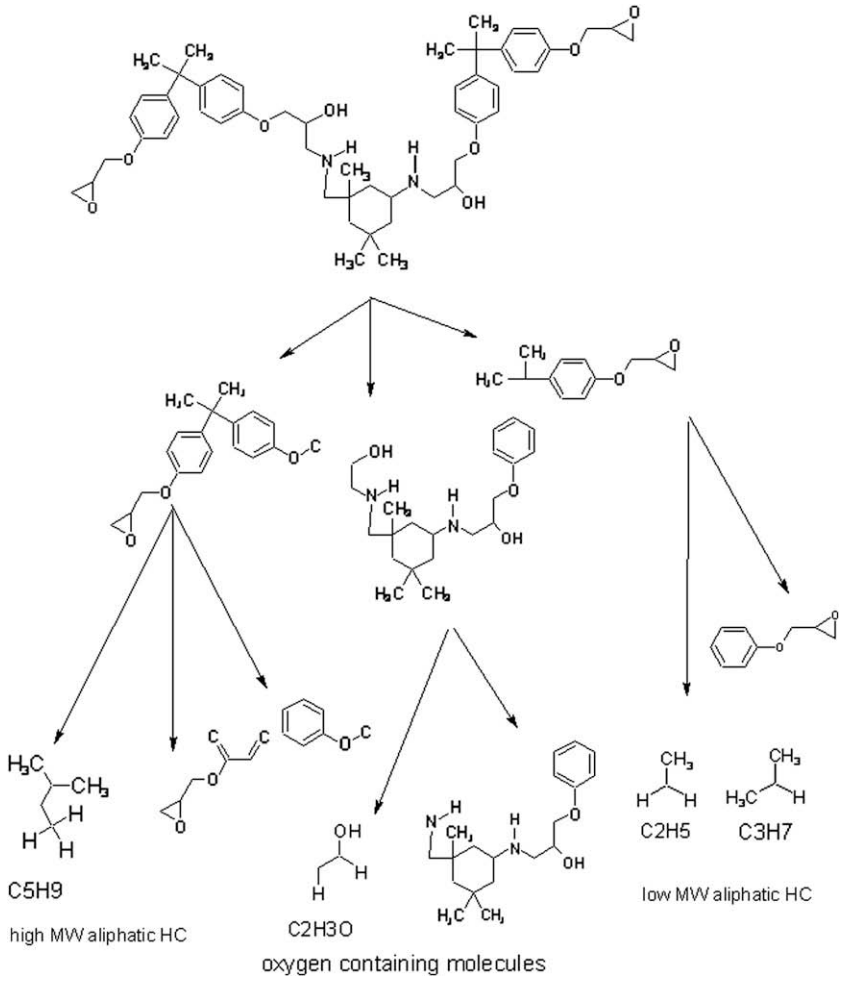

Fig. 4. Proposed chain scission reaction of DGEBA/IPD cured resin matrix according to one theme extracted from ToF-SIMS data.

relative ion intensity of the aliphatic hydrocarbon ions featured in Fig. 3a and b.

Comparison between Figs. 1a, 2a, 3a, and 3b indicates that the 3D and E-glass composites suffered significant chain scission and loss of network density and aliphatic hydrocarbon molecules as shown by the reduction in the relative ion intensity of the $C_3H_5^+$, $C_2H_5^+$, $C_3H_7^+$ and $C_2H_3^+$ ions between the untreated and the treated samples. On the other hand, CF composite samples showed resilience under the treatment conditions; in fact, a slight increase in the aliphatic hydrocarbon ion count is observed. This may be due to the experimental conditions inducing a slight cross-linking reaction with the support of species migrating to the surface from the filler in the subsurface. Other explanation might be the generation of a heat-induced condensation reaction, forming polyaromatic structures at the surface [37].

The other significant group of ions in PC1 contains $C_2H_3O^+$, $C_3H_3O^+$ and $C_3H_7NO^+$. All samples exhibited treatment-induced oxidation of the surface as indicated by the rise in the oxygen content (as indicated by XPS earlier) and the increase in oxygen-containing molecules at the surface revealed by ToF-SIMS positive ion spectra (Fig. 3c). PC1 collected information related to this phenomenon. Fig. 3c shows that the oxygen-containing ions $C_2H_3O^+$, $C_3H_3O^+$ and $C_3H_7NO^+$ significantly increase in intensity as a result of the treatment for the 3D and E-glass composites but to a lesser extent for the CF composite. The extent of surface oxidation increases with the extent of chain scission, as expected. Fig. 3 shows that all treated samples have lower relative ion intensity of aliphatic hydrocarbons and higher oxygen and nitrogen containing ions in comparison with the untreated samples. An increase in chain openings and generation of reaction sites from chain scission creates more opportunities for the surrounding oxygen and nitrogen to bond with the epoxy chains, see Fig. 4. Fig. 5 shows a proposed oxidation reaction resulting from UV treatment of DGEBA/IPD epoxy resin. It is proposed that chain breakage facilitates the formation of oxygen rich end groups. The increase in oxidised end groups is detected by ToF-SIMS, oxygen and nitrogen containing ions in Fig. 3c, and depends largely on the extent of the chain scission reaction for each of the composites studied.

PC2 collected information that separated the CF composite sample from the rest of the samples, as shown in Fig. 1a. The untreated and treated glass composite samples overlapped with each other and no clear trend is observed. Hence, the information collected by PC2 is specifically influenced by the characteristics of the carbon fibre samples, with limited sensitivity for distinguishing untreated from treated CF samples.

The most significant ions that contribute to the PC2 loadings are the aliphatic hydrocarbon ions $C_3H_7^+$, $C_4H_9^+$, $C_4H_7^+$, $C_5H_9^+$, $C_5H_{11}^+$, that appear on one side of the loadings plot and $C_2H_3^+$, $C_3H_3^+$ and $C_3H_5^+$ appearing on the other side. There is also some contribution from the $C_3H_7NO^+$ ion. The CF composite is distinguished from the rest of the samples due to its significantly lower change in aliphatic hydrocarbon ion intensity as a result of the treatment. The different groups of aliphatic hydrocarbon ions that appear on opposite side of the loadings plot represent the two conflicting phenomena of

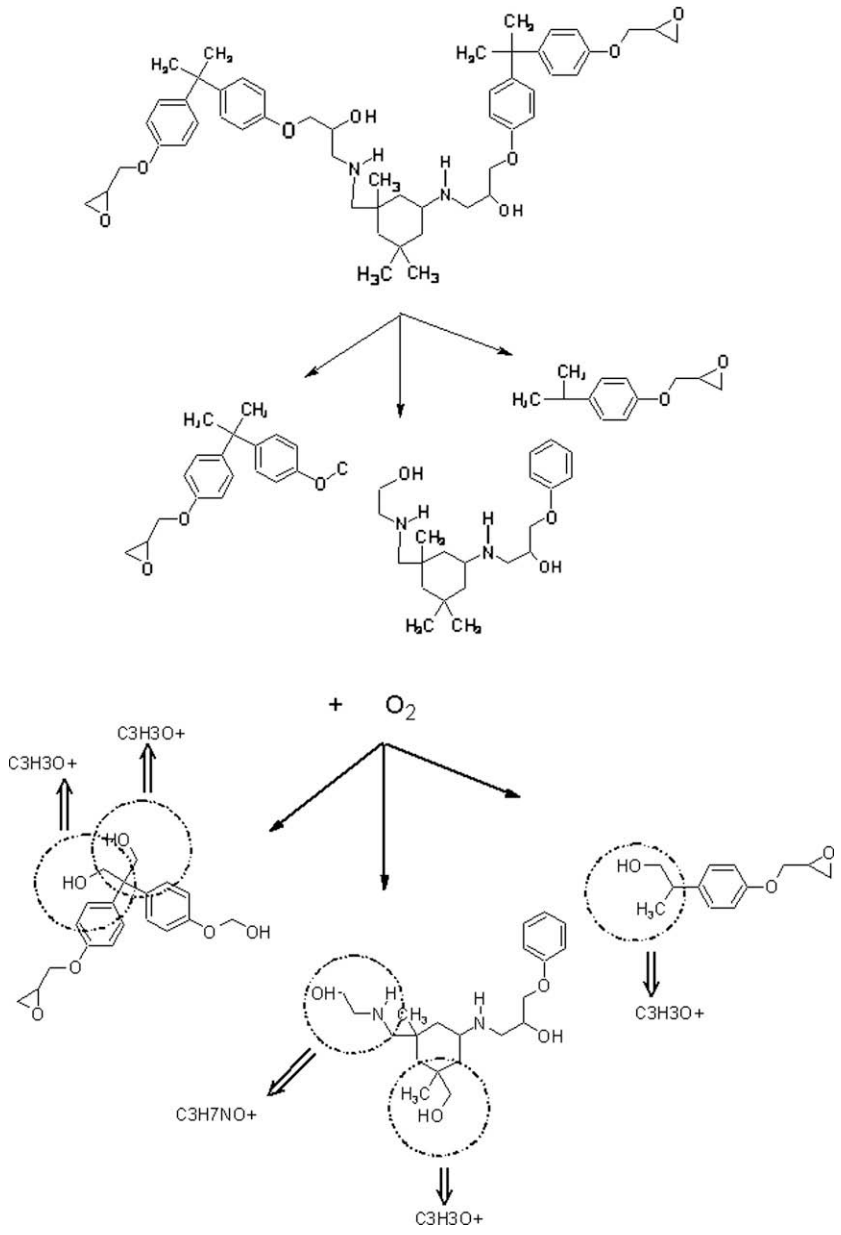

Fig. 5. Proposed oxidation reaction of DGEBA/IPD cured resin matrix according to one theme extracted from ToF-SIMS data.

chain cross-linking and chain scission. Chain scission reactions result in the release of low molecular weight aliphatic hydrocarbon groups, structures having three carbon atoms and less, which are indicated by the reduction of relative ion intensity of the corresponding ions after UV treatment. On the other hand, chain cross-linking and condensation give rise to the aliphatic hydrocarbon ions with higher molecular weight (more than four carbon atoms) following UV treatment, as shown in Fig. 3b.

Fig. 1b shows the scores plot for PC3 vs PC4. These principal components, in combination, collected information that was sensitive enough to distinguish each sample from the others. However, there was some overlap between the CF-T and the 3D-T3 samples. The samples scores showed more scatter than the scores for PC1 and PC2 due to the effect of residual ion intensity from previous principal components. PC3 collected information that separated the untreated CF from the treated CF samples. Untreated and treated E-glass samples were also distinguished. There was no trend to establish between the 3D glass composites treated and untreated samples. There was also no clear trend to distinguish, on the whole, sample type or treatment effect. Fig. 2c shows that the aliphatic hydrocarbon ions $C_2H_3^+$, $C_2H_5^+$, $C_3H_3^+$, $C_3H_5^+$, and $C_5H_9^+$ are the major contribution. There is some contribution also from the $C_2H_3O^+$ and $C_3H_7NO^+$ ions. PC3 collects information regarding the extent of chain scission and the loss of low molecular weight aliphatic hydrocarbon molecules (corresponding ions are $C_2H_3^+$, $C_2H_5^+$, $C_3H_3^+$ and $C_3H_5^+$), which differ between samples. PC3 also collected residual effects from the oxidation reaction through the acquiring of the variance of the oxygen-containing ions.

PC4 distinguished two groups of samples that overlapped within the group, Fig. 1b. Fig. 2d shows that the ions that contribute mostly to the PC4 loadings plot are $C_3H_5^+$, $C_3H_3^+$, $C_2H_5^+$, $C_4H_{10}^+$ and $C_3H_7NO^+$. PC4 collected residual effects from the chain scission reaction ($C_3H_5^+$, $C_3H_3^+$, and $C_2H_5^+$), cross-linking/condensation reaction ($C_4H_{10}^+$) and oxidation reaction ($C_3H_7NO^+$).

Fig. 6 shows the PCA scores for the ToF-SIMS negative ion spectra. PC1 collected 88.9% of the total variance while PC2

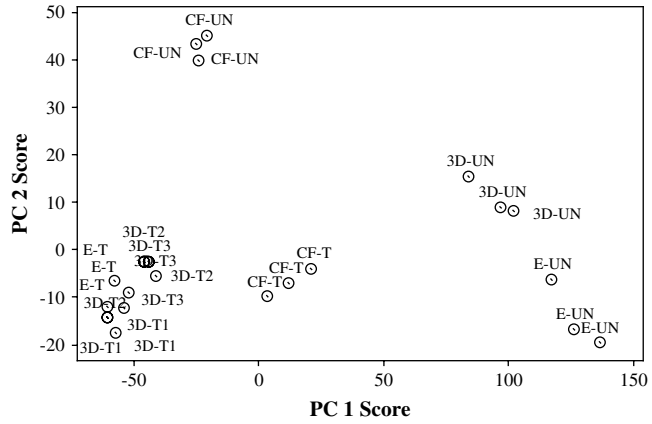

Fig. 6. Principal components analysis scores plots of the negative ToF-SIMS spectra for PC1 vs PC2 scores.

collected 6.4%. PC1 scores, shown in Fig. 6a, distinguish between the untreated and treated 3D glass and E-glass composites. They feature on the opposite side of the plot. PC1 also distinguishes between the untreated and the treated CF sample but at less scores variance than other composites. Hence, PC1 collects information that is directly related to the degradation of the composites.

The PC1 loadings plot, Fig. 7a, shows that the major ions contributing to PC1 variance are H^-, CNO^-, CN^-, and C_2H^-. Some contribution is also noticeable from $C_3H_3O_2^-$, CHO_2^-, $C_2H_2O_2^-$ and $C_4H_2O^-$. Fig. 8a and c shows that the relative intensity of the CN^- and CNO^- ions increases significantly after treatment for all

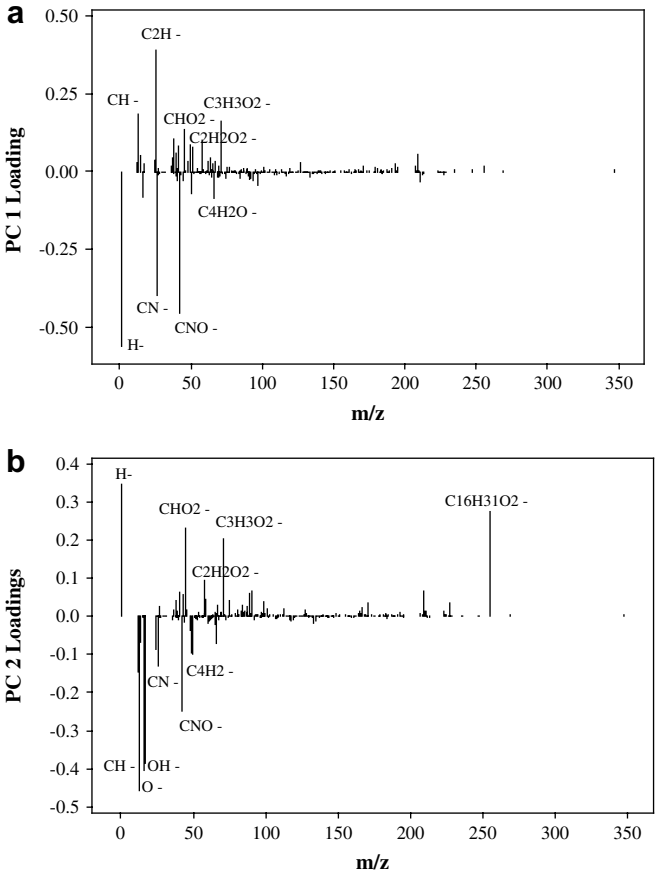

Fig. 7. Principal components analysis loadings plots for the ToF-SIMS negative spectra of (a) PC1, (b) PC2.

composites. The change in intensity of these ions appears more significant in the E-glass and 3D glass composite than the CF composite. This explains the position of the untreated CF sample in the scores plot. Hence, PC1 collected information regarding the oxidation of the epoxy resin composite samples.

In this study, the findings from both the positive and negative spectra indicate that the glass composites are more strongly oxidised than the CF composite in response to accelerated UV degradation conditions. This is a critical outcome. All samples have been fabricated with the same epoxy and the accepted position in composite science is that the reinforcing material is completely encapsulated by this epoxy. The experimental evidence, however, indicates that the type and behaviour of the reinforcement influences the degradation pathway.

PC2 scores, as shown in Fig. 6a, distinguish the CF-UN and the 3D-UN samples from the other samples. PC1 and PC2 scores, in combination, divide the sample set into five distinct groups. The untreated samples (3D glass, CF and E-glass) can all be separated. Of the treated samples, CF-T may be distinguished from the other two types.

The PC2 loadings plot, Fig. 5b, shows that the H-ion remains the main contributor to the variance. Other substantial contributions to PC2 arise from O^-, OH^-, $C_{16}H_{31}O_2^-$, CHO_2^-, and $C_3H_3O_2^-$ ions, with lesser contributions from CNO^-, CN^-, $C_2H_2O_2^-$ and the $C_4H_2^-$ ions.

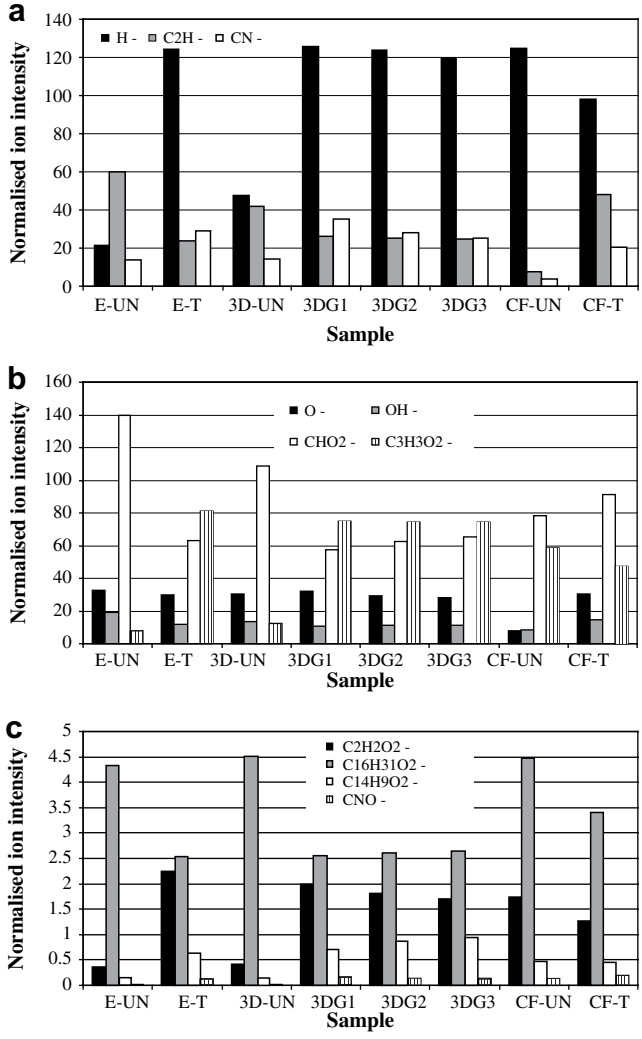

Fig. 8. Variation in the intensity of secondary ion peaks of the negative ToF-SIMS spectra that showed significant variance by PCA. Each bar represents the average of three readings of ion intensities with standard deviation.

The untreated CF composite sample has the least relative ion intensity of the O^- and OH^- ions compared with the other samples. This is a further indication of the difference in the surface oxidation between the three composites as a result of the UV accelerated degradation process. PC2 collected similar variance for the 3D and E-glass composites while CF samples generated different variance as shown from the relative ion intensities of the main ions contributed to PC2 in Fig. 6. This indicates the effect of filler on the epoxy resin surface response to UV treatment.

4. Conclusions

Epoxy resin composites fabricated with different reinforcement materials have been shown to have a different surface response to UV accelerated degradation conditions. XPS measurements showed that all epoxy resin composites suffered significant surface oxidation. The 3D glass sample showed the most significant increase of oxygen concentration at the surface; approximately 50%.

The E-glass, 3D glass and CF composites showed different relative ion intensity for aliphatic and oxygen-containing ions. Combining the ToF-SIMS positive and negative ion data with previous knowledge and XPS data indicated the occurrence of the chemical phenomena of chain scission, cross-linking/condensation and oxidation as a result of the accelerated degradation. However, these processes occurred at different rates in the three composites. PCA analysis of the ToF-SIMS positive ion spectra showed that PC1 collected information regarding the surface chain scission phenomena and oxidation. PC2 provided some insight into the occurrences of surface cross-linking in the CF composite. PCA analysis of the negative spectra provided information regarding the oxidation reaction on the surface of the degraded composites. It also provided further evidence on the different rates of surface oxidation among the different composites.

Although this study clearly reveals that the nature of the reinforcement affects the epoxy resin composite response to UV degradationthe reasons behind such behaviour are still not completely resolved. Further studies should focus on the nature of the different reinforcement/epoxy interaction.

Acknowledgements

The authors gratefully acknowledge the input of Francesca Bennet and Christopher Barner-Kowollik of the Centre for Advanced Macromolecular Design, University of New South Wales in accelerated degradation trials, and Robert Jones of the Centre for Materials and Surface Science, La Trobe University in XPS and ToF-SIMS data acquisition.

The authors also acknowledge the financial assistance of the Australian Research Council and the State Government of Victoria Science, Technology and Innovation Initiative in the acquisition of XPS and ToF-SIMS instrumentation.

References

[1] Peters ST. Handbook of composites. Chapman and Hall; 1998.
[2] Kelly V. Carbon fibre, manufacture and application. Elsevier; 2004.
[3] Aird F. Fiberglass and composite materials. Berkley Publishing Company; 1996.
[4] Iskanderova Z, Kleiman J, Gudimenko Y, Tennyson RC, Morison WD. Comparison of surface modification of polymeric materials for protection from severe oxidative environments using different ion sources. Surf Coat Technol 2000;127:18–23.
[5] Han J, Kim C. Low earth orbit space environment simulation and its effects on graphite/epoxy composites. Compos Struct 2006;72:218–26.
[6] Olivier L, Baudet C, Bertheau D, Grandidier JC, Lafarie-Freno, MC. Development of experimental, theoretical and numerical tools for studying thermo-oxidation of CFRP composites. Compos Part A Appl S, in press, doi: 10.1016/j.compositesa.2008.04.005.
[7] Ciutacu S, Budrugeac P, Niculae I. Accelerated thermal aging of glass--reinforced epoxy resin under oxygen pressure. Polym Degrad Stab 1991;31:365–72.
[8] Lafarie-Frenota MC, Rouquiéa S, Hoa NQ, Bellenger V. Comparison of damage development in C/epoxy laminates during isothermal ageing or thermal cycling. Compos Part A Appl S 2006;37:662.
[9] Decelle J, Huet N, Bellenger V. Oxidation induced shrinkage for thermally aged epoxy networks. Polym Degrad Stab 2003;81:239–48.
[10] Dry C. Procedures developed for self-repair of polymer matrix composite materials. Compos Struct 1996;35:263.
[11] Pang JWC, Bond IP. A hollow fibre reinforced polymer composite encompassing self-healing and enhanced damage visibility. Compos Sci Technol 2005;65:1791–9.
[12] Niezgoda T, Barnat W. Analysis of protective structures made of various composite materials subjected to impact. Mater Sci Eng A 2008;483:705–7.
[13] Abrate S. Impact on composite structures. Cambridge, UK: Cambridge University Press; 1998.
[14] Hancox NL. Thermal effects on polymer matrix composites. Part 1. Thermal cycling. Mater Des 1998;19:85–91.
[15] Aymerich F, Priolo P, Sun CT. Static and fatigue behavior of stitched graphite/epoxy composite laminates. Int J Fract 2003;63:907–17.
[16] Bénard Q, Fois M, Grisel M. Influence of fibre reinforcement and peel ply surface treatment towards adhesion of composite surfaces. Int J Adhes Adhes 2005;25:404–9.
[17] Ray BC. Temperature effect during humid ageing on interfaces of glass and carbon fibers reinforced epoxy composites. J Colloid Interface Sci 2006;298:111–7.
[18] Greenhalgh E, Bishop SM, Bray D, Hughes D, Lahiff S, Millson B. Characterisation of impact damage in skin-stringer composite structures. Compos Struct 1996;36:187–207.
[19] Chaturvedi M, Shen YL. Thermal expansion of particle-filled plastic encapsulant: a micromechanical characterization. Acta Mater 1998;46(12):4287–302.
[20] Wagner MS, Ratner BD, Castner DG. Maximizing information obtained from secondary ion mass spectra of organic thin films using multivariate analysis. Surf Sci 2004;570:78–97.
[21] Graham DJ, Wagner MS, Castner DG. Information from complexity: challenges of TOF-SIMS data interpretation. Appl Surf Sci 2006;252:6860–8.
[22] Gradowski M, Jacoby TB, Hilgers H, Barz J, Wahl M, Kopnarski M. ToF-SIMS characterisation of ultra-thin fluorinated carbon plasma polymer films. Surf Coat Technol 2005;200:334–40.
[23] Gardella Jr JA, Mahoney CM. Determination of oligomeric chain length distributions at surfaces using ToF-SIMS: segregation effects and polymer properties. Appl Surf Sci 2004;231–232:283–8.
[24] Oran U, Nveren EU, Wirth T, Unger WES. Poly-dimethyl-siloxane (PDMS) contamination of polystyrene (PS) oligomers samples: a comparison of time-of-flight static secondary ion mass spectrometry (TOF-SSIMS) and X-ray photoelectron spectroscopy (XPS) results. Appl Surf Sci 2004;227:318–24.
[25] Médard N, Aouinti M, Poncin-Epaillard F, Bertrand P. ToF-SIMS ability to quantify surface chemical groups: correlation with XPS analysis and spectrochemical titration. Surf Interface Anal 2001;31:1042–7.
[26] Eynde XV, Bertrand P. Combined XPS and ToF-SIMS study of miscible polymer blend surfaces: polystyrene/poly(2,6-dimethyl-1,4-phenylene oxide) (PS/PDMPO). Surf Interface Anal 1999;27:157–64.
[27] Kim Y, Lee YT, Han S, Kim K. Improvement of hydrophobic properties of polymer surfaces by plasma source ion implantation. Surf Coat Technol 2006;200:4763–9.
[28] Mutel B, Grimblot J, Dessaux O, Goudmand P. XPS investigations of nitrogen-plasma-treated polypropylene in a reactor coupled to the spectrometer. Surf Interface Anal 2000;30:401–6.
[29] Coullerez G, Leonard D, Lundmark S, Mathieu H. XPS and ToF-SIMS study of freeze-dried and thermally cured melamine-formaldehyde resins of different molar ratios. Surf Interface Anal 2000;29:431–43.
[30] Rattana A, Abel ML, Watts JF. ToF-SIMS studies of the adsorption of epoxy resin molecules on organosilane-treated aluminium: adsorption kinetics and adsorption isotherms. Int J Adhes Adhes 2006;26:28.
[31] Treverton JA, Paul AJ, Vickerman JC. Characteristics of adhesive and coating constituents by time-of-flight secondary ion mass spectrometry (ToF-SIMS). Surf Interface Anal 1993;30:449–56.
[32] Woerdeman DL, Parnas RS, Giunta RK, Wilkerson AL. Dewetting of unreacted epoxy/amine mixtures on silica. J Colloid Interface Sci 2002;249:246–52.
[33] Martens H, Naes T. Multivariate calibration. London: Wiley; 1989.
[34] Lee WH, Lee JG, Reucroft PJ. XPS study of carbon fiber surfaces treated by thermal oxidation in a gas mixture of $O2/(O2+N2)$. Appl Surf Sci 2001;171:136–42.
[35] Kim MH, Rhee KY, Kim HJ, Jung DH. Surface modification of carbon/epoxy prepreg using oxygen plasma and its effect on the delamination resistance behavior of carbon/epoxy composites. Mater Sci Eng A – Struct 2007;448:269–74.
[36] Awaja F, van Riessen G, Fox B, Kelly G, Pigram PJ. Tof-SIMS investigation of epoxy resin curing reaction at different rein to hardener ratio. J Appl Polym Sci 2008;110:2711–7.
[37] Rose N, La Bras M, Delobal R, Cosles B, Henry Y. Thermal oxidative degradation of an epoxy resin. Polym Degrad Stab 1993;42:307–16.